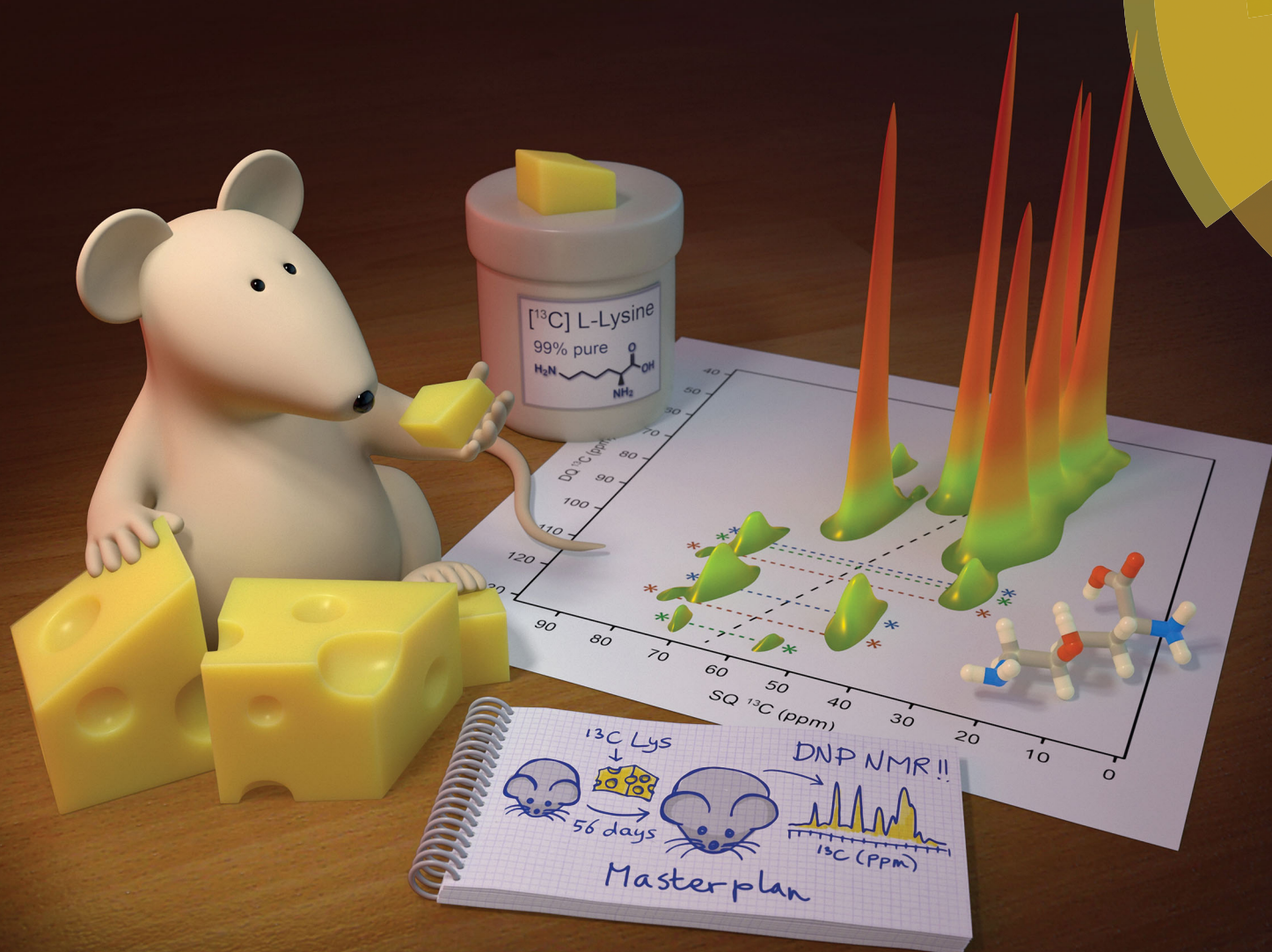


# ChemComm

Chemical Communications

rsc.li/chemcomm



ISSN 1359-7345



## COMMUNICATION

Hartmut Oschkinat, Melinda J. Duer *et al.*

Essential but sparse collagen hydroxylysyl post-translational modifications detected by DNP NMR



Cite this: *Chem. Commun.*, 2018, **54**, 12570

Received 21st June 2018,  
Accepted 2nd October 2018

DOI: 10.1039/c8cc04960b

rsc.li/chemcomm

## Essential but sparse collagen hydroxylysyl post-translational modifications detected by DNP NMR†

Wing Ying Chow,<sup>a</sup> Rui Li,<sup>b</sup> Ieva Goldberga,<sup>b</sup> David G. Reid,<sup>b</sup> Rakesh Rajan,<sup>b</sup> Jonathan Clark,<sup>c</sup> Hartmut Oschkinat,<sup>\*a</sup> Melinda J. Duer,<sup>\*b</sup> Robert Hayward<sup>d</sup> and Catherine M. Shanahan<sup>d</sup>

**The sparse but functionally essential post-translational collagen modification 5-hydroxylysine can undergo further transformations, including crosslinking, O-glycosylation, and glycation. Dynamic nuclear polarization (DNP) and stable isotope enriched lysine incorporation provide sufficient solid-state NMR sensitivity to identify these adducts directly in skin and vascular smooth muscle cell extracellular matrix (ECM), without extraction procedures, by comparison with chemical shifts of model compounds. Thus, DNP provides access to the elucidation of structural consequences of collagen modifications in intact tissue.**

Lysine modifications are critical to collagen ECM structure, function, and properties.<sup>1,2</sup> These usually start with hydroxylation at the  $\delta$ -(*i.e.* the 5-) carbon and lead to a cascade of reactions that generate diverse chemical structures. The modifications can be enzymatically-driven as part of collagen and ECM biosynthesis, but can also occur without enzymatic involvement in conditions such as diabetes, cancer and ageing. Interruption of the lysine modification process may lead to embryonic and perinatal lethality in mouse, and osteogenesis imperfecta and Ehler-Danlos disease in humans.<sup>1,3</sup> Being able to observe such lysine modifications in tissues without the application of extraction procedures is critical for understanding their physiological necessity, as well as the role they play in pathological and degradation processes.

Lysyl hydroxylases<sup>4</sup> modify C<sub>5</sub> in less than 2%<sup>5</sup> of lysine residues in collagen to yield (R)-5-hydroxylysine (Hyl). Hyl residues are critical sites for further modifications, including their

attachment to other Lys residues in a variety of cross-links,<sup>6,7</sup> (ESI,† Schemes S1 and S2), adduction of sugar species *via* specific and essential enzymatic glycosylation,<sup>8,9</sup> (ESI,† Scheme S3), and invariably deleterious spontaneously occurring glycation<sup>10,11</sup> (ESI,† Scheme S4). The generation of Hyl and all three types of subsequent modifications will produce broadly predictable changes in the NMR spectra of ECM materials; the challenge is detecting these low abundance species against an overwhelming background of irrelevant signals.

Conventional analysis of collagen modifications relies on mass spectrometry.<sup>12–14</sup> The identification procedure demands many, often chemical, pre-treatments.<sup>15,16</sup> While sensitive and potentially quantitative, these approaches are destructive and raise the possibility of side reactions or degradation during processing. There is a need to develop complementary analytical techniques to arrive at a full picture of the identity and quantity of collagen modifications in a range of biological samples.

Solid-state NMR (ssNMR) offers the possibility of identifying such collagen modifications in intact tissue without extensive processing or purification. With ssNMR, the types of species present may be identified, and valuable structural and dynamical information on crosslinked, glycosylated and glycated sites within intact ECM may be obtained. A significant challenge in this approach is the relatively low sensitivity of solid-state NMR spectroscopy, exacerbated by the low natural abundance of NMR-active nuclei and the fact that the residues of interest occur at levels well under 2% of all residues found in collagen proteins.

The strategy applied here combines stable isotopic labelling with NMR signal enhancement by DNP.<sup>17–19</sup> To show the wide applicability of this strategy, two different kinds of samples were investigated: skin obtained from mice fed a (U-<sup>13</sup>C<sub>6</sub>)-lysine diet, and ECM generated by vascular smooth muscle cell (VSMC) culture as a potential *in vitro* model with relevance to vascular diseases. Labelling with NMR-active stable isotopes (*e.g.* <sup>13</sup>C, <sup>15</sup>N) is a well-established procedure for enhancing sensitivity and information content.<sup>20,21</sup> We have developed cell culture methods for generating labelled ECM by supplementing growth media

<sup>a</sup> Leibniz Forschungsinstitut für Molekulare Pharmakologie, Campus Buch, Robert-Rössle Str. 10, Berlin 13125, Germany. E-mail: oschkinat@fmp-berlin.de; Tel: +49 30 94793 160

<sup>b</sup> Department of Chemistry, University of Cambridge, Lensfield Road, Cambridge CB2 1EW, UK. E-mail: mjd13@cam.ac.uk; Fax: +44 1223 336362; Tel: +44 1223 736394

<sup>c</sup> Babraham Institute, Babraham Research Campus, Cambridge CB22 3AT, UK

<sup>d</sup> BHF Centre of Research Excellence, Cardiovascular Division, King's College London, London SE5 9NU, UK

† Electronic supplementary information (ESI) available. See DOI: 10.1039/c8cc04960b

with isotope-enriched amino acids.<sup>22</sup> A dietary approach is particularly effective for labelling mice in essential amino acids like lysine, where incorporation from diet is not in competition with *de novo* native biosynthesis.<sup>23</sup> Accordingly,  $^{13}\text{C}$ -enriched murine skin was obtained by direct feeding of mice with ( $\text{U-}^{13}\text{C}_6$ )-lysine, while VSMC ECM<sup>24</sup> was labelled using growth medium supplemented with ( $\text{U-}^{13}\text{C}_6$ ,  $^{15}\text{N}_2$ )-lysine. Note that the dietary approach does not completely isotope enrich the experimental animal as tissue biosynthesis and turnover can vary; we achieved 45%  $^{13}\text{C}$ -lysine enrichment on mouse skin.

The second component of our strategy to overcome the significant challenge of observing dilute molecular sites was to use DNP<sup>25</sup> to enhance signal sensitivity further. Despite the inhomogeneous signal broadening inevitable at cryogenic temperatures due to reduction of motional averaging, and the homogeneous signal broadening due to the presence of the radicals, the increased sensitivity from DNP enhancement renders weak signals observable that do not emerge above noise within a reasonable timeframe by conventional NMR. DNP has been usefully applied to large molecular systems, such as ribosomes,<sup>26</sup> and assembled HIV capsid proteins.<sup>27</sup> In a similar vein, we use DNP signal enhancement to probe sparse modifications of specifically labelled residues within intact collagen fibrils: large well-ordered, super-coiled, cross-linked units of triple-helical collagen, each around 300 kDa in molecular weight.

The  $^{13}\text{C}$ -Lys enriched samples are dry, solid biomaterials, hence we doped 10–15 mg of each with 17–20 mM AMUPol<sup>28</sup> dissolved in water (75%  $\text{D}_2\text{O}$ , 25%  $\text{H}_2\text{O}$ ), centrifuged the added radical solution several times in the rotor, and incubated the rotor in the fridge. This procedure resembles the incipient wetness impregnation technique as applied to porous materials.<sup>29</sup>

In contrast to common practice in DNP-NMR, glycerol was not added as it modifies collagen stability.<sup>30</sup> Mouse skin samples do exhibit up to 50% higher enhancements with glycerol (ESI,† Fig. S1), however, the VSMC ECM sample without glycerol showed higher enhancement than the glycerol-containing mouse skin sample. Furthermore, glycerol addition leads to artefacts in the same region as the Hyl signals (ESI,† Fig. S2). Considering the potential structural complications, and as Hyl signals can already be observed in both samples without glycerol, we omitted it for the rest of this study.

DNP enhancements of  $26.5 \pm 1.5$  for skin and  $57 \pm 4$  for VSMC ECM were measured by comparing microwave-on *versus* microwave-off 1D  $^{13}\text{C}$  MAS NMR spectra. The error is obtained by calculating the average enhancement of the most (generally  $\text{C}_\alpha$ ) and the least (generally  $\text{C}_\beta/\text{C}_\gamma$ ) enhanced signals (ESI,† Fig. S1), indicating uniform DNP enhancements. Taking possible depolarization effects of up to 60% into account,<sup>31</sup> these enhancements represent one to two orders of magnitude reduction in NMR signal averaging time. All experiments were carried out at 110 K, the lowest temperature where we have the required long-term stability to complete the NMR experiments.

As expected, the 1D  $^{13}\text{C}$  CP DNP NMR spectra of the isotope enriched skin and VSMC ECM are dominated by signals from unmodified Lys in collagen<sup>32</sup> and other proteins (ESI,† Fig. S2). Cross peaks in 2D dipolar assisted rotational resonance (DARR)<sup>33</sup> spectra (Fig. 1A and ESI,† Fig. S2, S3) reveal proximal  $^{13}\text{C}$ - $^{13}\text{C}$  pairs. While the most intense signals arise from Lys residues, three distinct Hyl-derived spin systems can be resolved in the DARR spectra, highlighted in Fig. S2 (ESI†) (red boxes) and detailed in Fig. 1A. As these signals can only arise from derivatives of  $^{13}\text{C}$ -enriched Lys, they must correspond to Lys post-translational modifications.

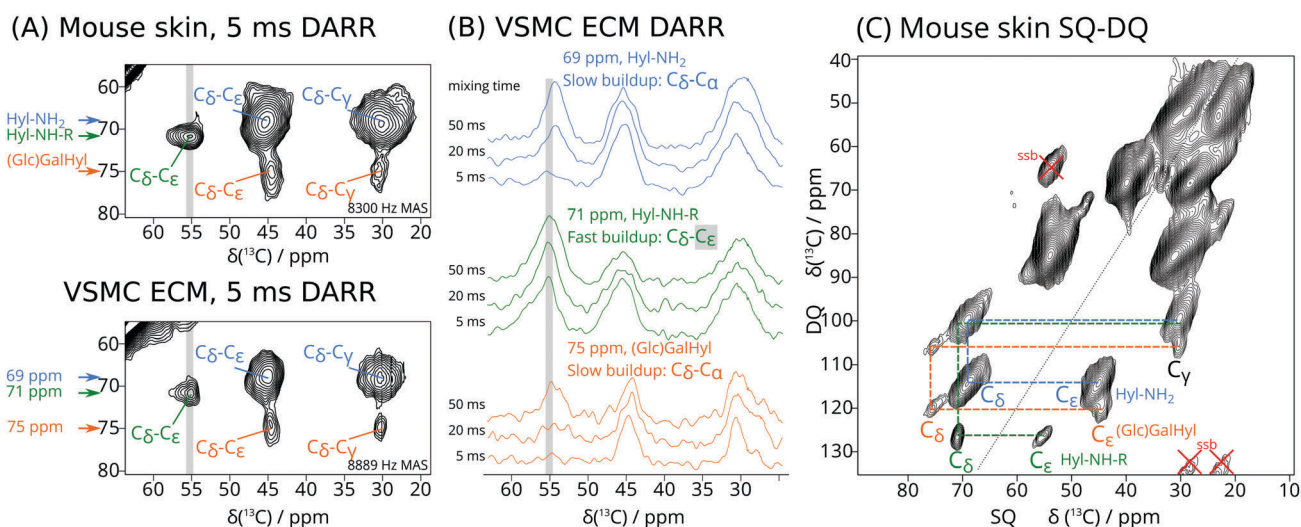


**Fig. 1** (A) Regions of 2D  $^{13}\text{C}$ - $^{13}\text{C}$  DARR NMR spectra (5 ms mixing time, 110 K) of  $\text{U-}^{13}\text{C}_6$  Lys labelled skin (15 mg, 8300 Hz MAS, acquisition 17 h, top) and VSMC ECM (15 mg, 8889 Hz MAS, acquisition time 7 h, bottom) showing cross peaks between Hyl  $\text{C}_\delta$  and other  $^{13}\text{C}$ -labelled carbons in Hyl and its derivatives. Blue annotations at 69 ppm ( $F_1$ ) depict underivatized Hyl (Hyl-NH<sub>2</sub>), green annotations at 71 ppm ( $F_1$ ) modified Hyl likely due to crosslinks and/or glycation (Hyl-NH-R), and orange annotations at 75 ppm ( $F_1$ ) glycosylated Hyl ((Glc)GalHyl). (B) Traces taken from DARR correlations of labelled VSMC ECM at different DARR mixing times, showing intensity changes of cross peaks involving Hyl  $\text{C}_\delta$ . The rapid build-up of the correlation with the  $\text{C}_\epsilon$  signal of Hyl-NH-R (green traces) at 56 ppm indicates that this signal can be distinguished from the correlation to the more distant Hyl  $\text{C}_\alpha$  at 54 ppm, which builds up more slowly. (C) 2D  $^{13}\text{C}$ - $^{13}\text{C}$  SQ-DQ NMR spectrum of labelled skin, showing the same Hyl  $\text{C}_\delta$ - $\text{C}_\epsilon$  signal that we have identified in (A) and (B).





Specifically, the cross peaks in Fig. 1A are consistent with Hyl and its derivatives, with the signals of the hydroxylated C $\delta$  around 70 ppm. The largest signals, centred at 69 ppm, likely correspond to Hyl residues that have not undergone further modification and show good agreement with solution-state NMR chemical shifts (see ESI $^\dagger$ ), thus we refer to this set of signals as **Hyl-NH $_2$** . A set of weaker but distinct signals at 75 ppm is consistent with *O*-glycosylated Hyl, in line with solution-state NMR shifts of GalHyl<sup>34,35</sup> and GlcGalHyl,<sup>35,36</sup> thus we refer to it as **(Glc)Gal-Hyl** (ESI $^\dagger$ , Scheme S3), though we note that we are unable to determine whether Hyl is glycosylated with GlcGal or only Gal at this stage. We expect these signals to be weaker since only up to one third of all Hyl is glycosylated. The well-resolved cross peak at 71 ppm (F $_1$ ) and 56 ppm (F $_2$ ) is consistent with a C $\delta$ -C $\epsilon$  cross peak for Hyl derivatized at N $\zeta$  (see ESI $^\dagger$  for reference model structures), which we term **Hyl-NH-R**. The rapid build-up of the **Hyl-NH-R** cross peak at 71–56 ppm (Fig. 1B green traces) distinguishes it from the overlapping but more slowly increasing signal corresponding to the **Hyl-NH $_2$**  C $\delta$ -C $\alpha$  correlation, for which the cross peak occurs at 69 ppm F $_1$  and 54 ppm F $_2$  (Fig. 1B blue traces). This effect is especially apparent in the traces from spectra recorded with DARR mixing times of 5 ms (Fig. 1B). From this result, we can deduce that the 71–56 ppm cross peak arises from two carbons that are directly bonded to each other. The signals around 70 ppm are due to Hyl C $\delta$ , thus the 56 ppm signal is identified as C $\epsilon$  by elimination. The SQ-DQ spectrum (Fig. 1C), where one-bond correlations dominate, provides further evidence of this pair of atoms, where we observed the 71–56 ppm correlation occurring at the expected DQ (sum) frequency of 127 ppm.

For Hyl without further modifications (**Hyl-NH $_2$** ), C $\epsilon$  occurs at 45 ppm. However, we can expect that substitutions at the Hyl N $\zeta$  primary amino group would shift the C $\epsilon$  signal about 10 ppm to higher frequency, thus providing a rationale for identifying the 56 ppm signal as C $\epsilon$  of **Hyl-NH-R**. Therefore, the **Hyl-NH-R** signal may represent Hyl modifications such as early glycation adducts, for instance with the C-1 of 1-deoxyfructose derived from glucose (ESI $^\dagger$ , Scheme S4). It may also correspond to enzymatically derived ketoamine crosslinks (*e.g.* HLKLN in ESI $^\dagger$ , Scheme S2). Chemical shifts in Table 1 are consistent with those of appropriate model compounds.<sup>34–36</sup> While the conventional aldimine structural formulation of immature aldimine cross links (*e.g.* deH-HLNL in ESI $^\dagger$ , Scheme S2) predicts a signal at 160–165 ppm for the  $\epsilon$ -imino carbon derived U- $^{13}\text{C}_6$  allysine, such signals were not observed.

Independent evidence that  $^{13}\text{C}$  signals around 70 ppm are due to Hyl C $\delta$  and its derivatives comes from heteronuclear

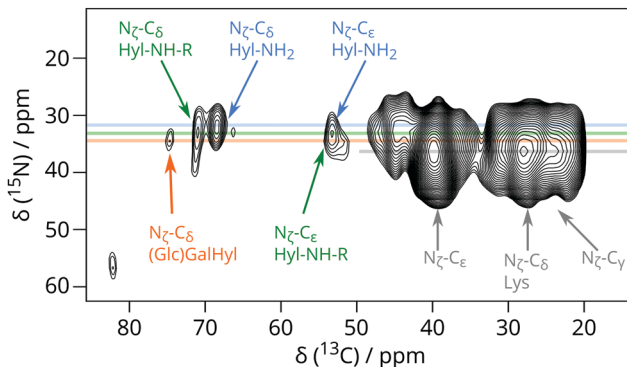


Fig. 2 Detail from  $^{15}\text{N}$ - $^{13}\text{C}$  correlation DNP-NMR experiment showing the correlation between Hyl C $\delta$  and Hyl N $\zeta$  signals for (U- $^{13}\text{C}_6$ ,  $^{15}\text{N}_2$ )-Lys enriched VSMC. This experiment took 51 hours.

correlations involving Hyl  $^{15}\text{N}_\zeta$  in the (U- $^{13}\text{C}_6$ ,  $^{15}\text{N}_2$ )-Lys enriched VSMC (Fig. 2 and Fig. S4, ESI $^\dagger$ ). Fig. 2 shows the region centred at 38 ppm  $^{15}\text{N}$  chemical shift corresponding to the Lys or Hyl 6-amino (N $\zeta$ ) group. The magnetisation evolved on  $^{15}\text{N}$  (Lys/Hyl N $\zeta$ ) was transferred to neighbouring C $\epsilon$ , and then further down the carbon skeleton by DARR mixing to the hydroxylated C $\delta$  around 70 ppm  $^{13}\text{C}$  chemical shift, resulting in a correlation connecting Hyl N $\zeta$  (38 ppm) to the corresponding C $\delta$  (69–71 ppm).

In summary, combining Lys isotope labelling and DNP enhancement enabled solid-state NMR observation of Hyl and other post-translational modifications in freeze-dried but otherwise intact collagenous ECM. We identified those due to *O*-glycosylated Hyl and signals indicative of *N*-adducts that correspond to early glycation products and/or crosslinks. These were present at levels of only a few percent of total Lys; we have thus conclusively shown that detection of these low abundance species within biologically-produced materials is possible without substantial extraction or purification. Our study attests to the potential of combining specific labelling and DNP to study the structural roles of Hyl in more complex organic-inorganic biocomposites such as bone<sup>22,37</sup> and pathological vascular calcifications.<sup>38</sup> The similarity of Hyl and derivatives between mammalian VSMC ECM generated by cell culture and native mouse skin supports our use of *in vitro* biomaterials as convenient and ethical model systems amenable to isotope labelling, in which the post-translational modification machinery is functioning faithfully. We are currently identifying the species adducted to Hyl using  $^{13}\text{C}$ -enriched sugar precursors, and increasing the proportions of  $^{13}\text{C}$ -labelled Lys and Hyl in our ECM to characterize cross links in more detail and under biologically relevant conditions. We envisage that such NMR-based techniques will be central in understanding the structural roles of Hyl and its modifications at the atomic level, to further our understanding of their physiological necessity in healthy tissue, and the part they play in disease and ageing.

Funding from the U.K. Medical Research Council for DGR and RR (grant RG75828), the SENS Foundation for JC, the Engineering and Physical Sciences Research Council for PhD studentships for RL and IG, postdoctoral fellowship funding

Table 1  $^{13}\text{C}$  Chemical shifts (ppm) of lysyl PTMs observed by DNP-NMR in collagen ECMs. Percentages represent abundances relative to Lys, estimated by volume integration of 5 ms mixing time DARR C $\delta$ -C $\epsilon$  cross peaks

PTM	C $\alpha$	C $\beta$	C $\gamma$	C $\delta$	C $\epsilon$	%Skin	%VSMC
Lys	54	30	23	28	40	100	100
Hyl ( <b>Hyl-NH<math>_2</math></b> )	54	28	30	69	45	14	7
Cross links/glycation ( <b>Hyl-NH-R</b> )	54	30	28	71	56	3	4
(Glc)GalHyl	54	28	30	75	44	3	2



from the DAAD and Leibniz Association for WYC, the CSC Cambridge Scholarship for PhD studentship for RL, and support by iNEXT, grant number 653706, funded by the Horizon 2020 programme of the European Commission.

## Conflicts of interest

There are no conflicts of interest. Animal procedures complied with institutional ethical guidelines, and the U.K. Animals (Scientific Procedures) Act 1986.

## Notes and references

- 1 J. Myllyharju and K. I. Kivirikko, *Trends Genet.*, 2004, **20**, 33.
- 2 K. Takaluoma, M. Hyry, J. Lantto, R. Sormunen, R. A. Bank, K. I. Kivirikko, J. Myllyharju and R. Soininen, *J. Biol. Chem.*, 2007, **282**, 6588.
- 3 K. Rautavuoma, K. Takaluoma, R. Sormunen, J. Myllyharju, K. I. Kivirikko and R. Soininen, *Proc. Natl. Acad. Sci. U. S. A.*, 2004, **101**, 14120.
- 4 M. Yamauchi and M. Sricholpech, *Essays Biochem.*, 2012, **52**, 113.
- 5 J. Myllyharju, *Collagen*, 2005, **247**, 115.
- 6 D. R. Eyre, M. A. Paz and P. M. Gallop, *Annu. Rev. Biochem.*, 1984, **53**, 717.
- 7 D. R. Eyre, I. R. Dickson and K. Van Ness, *Biochem. J.*, 1988, **252**, 495.
- 8 M. Sricholpech, I. Perdivara, M. Yokoyama, H. Nagaoka, M. Terajima, K. B. Tomer and M. Yamauchi, *J. Biol. Chem.*, 2012, **287**, 22998.
- 9 M. Terajima, I. Perdivara, M. Sricholpech, Y. Deguchi, N. Pleshko, K. B. Tomer and M. Yamauchi, *J. Biol. Chem.*, 2014, **289**, 22636.
- 10 A. G. Huebschmann, J. G. Regensteiner, H. Vlassara and J. E. B. Reusch, *Diabetes Care*, 2006, **29**, 1420.
- 11 V. M. Monnier, G. T. Mustata, K. L. Biemel, O. Reihl, M. O. Lederer, Z. Y. Dai and D. R. Sell, *Ann. N. Y. Acad. Sci.*, 2005, 533.
- 12 A. Naba, O. M. T. Pearce, A. Del Rosario, D. Ma, H. Ding, V. Rajeeve, P. R. Cutillas, F. R. Balkwill and R. O. Hynes, *J. Proteome Res.*, 2017, **16**, 3083.
- 13 W. Y. Jiang, B. Y. Zhou, G. L. Yu, H. Liu, J. B. Zeng, Q. D. Lin, H. L. Xi and H. Liang, *Biochem. Genet.*, 2012, **50**, 34.
- 14 I. Perdivara, M. Yamauchi and K. B. Tomer, *Aust. J. Chem.*, 2013, **66**, 760.
- 15 A. Kondo, O. Ishikawa, K. Okada, Y. Miyachi, S. Abe and Y. Kuboki, *Anal. Biochem.*, 1997, **252**, 255.
- 16 T. J. Sims, N. C. Avery and A. J. Bailey, *Methods Mol. Biol.*, 2000, **139**, 11.
- 17 K. K. Frederick, V. K. Michaelis, M. A. Caporini, L. B. Andreas, G. T. Debelouchina, R. G. Griffin and S. Lindquist, *Proc. Natl. Acad. Sci. U. S. A.*, 2017, **114**, 3642.
- 18 G. T. Debelouchina, M. J. Bayro, A. W. Fitzpatrick, V. Ladizhansky, M. T. Colvin, M. A. Caporini, C. P. Jaronec, V. S. Bajaj, M. Rosay, C. E. Macphee, M. Vendruscolo, W. E. Maas, C. M. Dobson and R. G. Griffin, *J. Am. Chem. Soc.*, 2013, **135**, 19237.
- 19 I. V. Sergeev, L. A. Day, A. Goldbourt and A. E. McDermott, *J. Am. Chem. Soc.*, 2011, **133**, 20208.
- 20 D. M. LeMaster, *Prog. Nucl. Magn. Reson. Spectrosc.*, 1994, **26**, 371.
- 21 J.-P. Demers, P. Fricke, C. Shi, V. Chevelkov and A. Lange, *Prog. Nucl. Magn. Reson. Spectrosc.*, 2018, **109**, 51.
- 22 W. Y. Chow, R. Rajan, K. H. Muller, D. G. Reid, J. N. Skepper, W. C. Wong, R. A. Brooks, M. Green, D. Bihan, R. W. Farndale, D. A. Slatyer, C. M. Shanahan and M. J. Duer, *Science*, 2014, **344**, 742.
- 23 V. W. C. Wong, D. G. Reid, W. Y. Chow, R. Rajan, M. Green, R. A. Brooks and M. J. Duer, *J. Biomol. NMR*, 2015, **63**, 119.
- 24 R. Li, R. Rajan, W. C. V. Wong, D. G. Reid, M. J. Duer, V. J. Somovilla, N. Martinez-Saez, G. J. L. Bernardes, R. Hayward and C. M. Shanahan, *Chem. Commun.*, 2017, **53**, 13316.
- 25 A. S. L. Thankamony, J. J. Wittmann, M. Kaushik and B. Corzilius, *Prog. Nucl. Magn. Reson. Spectrosc.*, 2017, **102–103**, 120.
- 26 S. Lange, W. T. Franks, N. Rajagopalan, K. Doring, M. A. Geiger, A. Linden, B. J. van Rossum, G. Kramer, B. Bukau and H. Oschkinat, *Sci. Adv.*, 2016, **2**, e1600379.
- 27 R. Gupta, M. Lu, G. Hou, M. A. Caporini, M. Rosay, W. Maas, J. Struppe, C. Suiter, J. Ahn, I. J. Byeon, W. T. Franks, M. Orwick-Rydmark, A. Bertarello, H. Oschkinat, A. Lesage, G. Pintacuda, A. M. Gronenborn and T. Polenova, *J. Phys. Chem. B*, 2016, **120**, 329.
- 28 C. Sauvee, M. Rosay, G. Casano, F. Aussenac, R. T. Weber, O. Ouari and P. Tordo, *Angew. Chem., Int. Ed.*, 2013, **52**, 10858.
- 29 A. Lesage, M. Lelli, D. Gajan, M. A. Caporini, V. Vitzthum, P. Mieville, J. Alauzun, A. Roussey, C. Thieuleux, A. Mehdi, G. Bodenhausen, C. Coperet and L. Emsley, *J. Am. Chem. Soc.*, 2010, **132**, 15459.
- 30 G. C. Na, *Biochemistry*, 1986, **25**, 967.
- 31 F. Mentink-Vigier, S. Paul, D. Lee, A. Feintuch, S. Hediger, S. Vega and G. De Paep, *Phys. Chem. Chem. Phys.*, 2015, **17**, 21824.
- 32 O. Nikel, D. Laurencin, S. A. McCallum, C. M. Gundberg and D. Vashishth, *Langmuir*, 2013, **29**, 13873.
- 33 K. Takegoshi, S. Nakamura and T. Terao, *Chem. Phys. Lett.*, 2001, **344**, 631.
- 34 P. Lamosa, L. O. Martins, M. S. Da Costa and H. Santos, *Appl. Environ. Microbiol.*, 1998, **64**, 3591.
- 35 P. Allevi, R. Paroni, A. Ragusa and M. Anastasia, *Tetrahedron: Asymmetry*, 2004, **15**, 3139.
- 36 P. Allevi, M. Anastasia, R. Paroni and A. Ragusa, *Bioorg. Med. Chem. Lett.*, 2004, **14**, 3319.
- 37 P. Zhu, J. Xu, N. Sahar, M. D. Morris, D. H. Kohn and A. Ramamoorthy, *J. Am. Chem. Soc.*, 2009, **131**, 17064.
- 38 M. J. Duer, T. Friscic, D. Proudfoot, D. G. Reid, M. Schoppet, C. M. Shanahan, J. N. Skepper and E. R. Wise, *Arterioscler., Thromb., Vasc. Biol.*, 2008, **28**, 2030.

